The Effect of 2-D Surface Irregularities on Laminar-Turbulent Transition: A Comparison of Numerical Methodologies

Francesco Tocci[1(✉)], Juan Alberto Franco[1], Stefan Hein[1], Guillaume Chauvat[2], and Ardeshir Hanifi[2]

[1] German Aerospace Center (DLR), Bunsenstrasse 10, 37073 Göttingen, Germany
francesco.tocci@dlr.de

[2] FLOW, Department of Engineering Mechanics, KTH Royal Institute of Technology, SE-100 44 Stockholm, Sweden

Abstract. The applicability of Local Stability Theory (LST), Parabolized Stability Equations (PSE) and the Adaptive Harmonic Linearized Navier-Stokes (AHLNS) approach is investigated in the presence of 2-D surface irregularities through comparison with Direct Numerical Simulations (DNS). Remarkably good agreement between DNS and AHLNS is obtained for the amplification curves of Tollmien-Schlichting (TS) waves in all the cases studied. The LST and PSE results exhibit differences which are discussed in relation to the local distortion of the boundary layer induced by the irregularities.

Keywords: Laminar-turbulent transition · 2-D surface irregularities · DNS · AHLNS · PSE · LST

1 Introduction

Laminar-turbulent transition prediction is of practical interest in aircraft design since transition affects important aerodynamic quantities such as drag and heat transfer. Extended laminar flow on aerodynamic surfaces is an effective way of reducing aircraft drag. One of the major challenges for the implementation of laminar-flow surfaces is the potential for any irregularity to move transition upstream. Under low-disturbance environment, boundary-layer transition results from the growth and breakdown of different flow instabilities. In 2-D flows the scenario is dominated by TS instabilities. Common wing-surface irregularities, such as two-dimensional steps, gaps or waviness can alter the growth characteristics of TS waves and therefore must be taken into account at the design stage [1]. The effect of steps, gaps and humps on the development of TS waves in an incompressible boundary layer has been investigated in [2] using DNS. All the irregularities were found to have an overall destabilizing effect. In the present work,

A. Dillmann et al. (Eds.): STAB/DGLR Symposium 2020, NNFM 151, pp. 246–256, 2021.
https://doi.org/10.1007/978-3-030-79561-0_24

we compare those results with LST, PSE and AHLNS. In the past, LST and PSE, together with the e^N method, have been successfully applied for transition prediction in cases without surface irregularities where the local streamwise flow gradients were small. However, the validity of the assumptions of such methods becomes questionable with the increased gradients locally induced by the surface irregularities. AHLNS removes some of the inherent limitations present in LST and PSE, and it has been already applied successfully in the presence of humps by Franco et al. [3]. Edelmann et al. [4] used DNS and LST with forward-facing steps introducing, for the latter, a special treatment in the region around the step and Park et al. [5] performed PSE analyses for smooth humps. To the best of the authors' knowledge, there is no published comparison between LST, PSE, AHLNS, and DNS for the development of TS waves encountering different types of surface irregularities.

2 Numerical Methods

In this section we present very brief descriptions of the numerical approaches used to study the linear spatial evolution of convective instabilities in boundary-layer flows. The instability of steady flows to small amplitude perturbations can be analysed using the modal approach. Given an operator that describes the evolution of small perturbations, this approach considers the temporal or spatial development of individual eigenmodes of that operator. The resulting linear stability theory relies on the decomposition of all flow quantities $\boldsymbol{q}$ into a steady basic flow $\overline{\boldsymbol{q}}$ plus an unsteady disturbance flow component $\tilde{\boldsymbol{q}}$ according to

$$\boldsymbol{q}(\boldsymbol{x},t) = \overline{\boldsymbol{q}}(\boldsymbol{x}) + \epsilon\tilde{\boldsymbol{q}}(\boldsymbol{x},t), \qquad \epsilon \ll 1, \tag{1}$$

where $\boldsymbol{x}$ is the space coordinate vector and t is time. Substituting (1) into the Navier-Stokes (NS) equations, subtracting the equations satisfied by the steady flow, and dropping the terms of order higher than ϵ yields the Linearized Navier-Stokes (LNS) equations. The basic laminar state $\overline{\boldsymbol{q}}$, around which the linearization is performed, needs to be calculated for each of the surface irregularities. In [2], the development of TS waves encountering a forward-facing step, backward-facing step, rectangular or smooth hump and gap was studied by means of DNS. That work provides the steady laminar 2-D basic flows for the instability analysis based on LST, PSE and AHLNS, which is the main contribution of this paper. Different assumptions can be made for the form of the basic flow and the disturbances in (1), which then result in the governing equations associated with LST, PSE and AHLNS. Due to space limitations, only the key aspects for each methodology are reported.

Local Stability Theory. In LST the flow is assumed to be parallel thus not accounting for the growth of the boundary layer. In the classical LST, the basic flow is considered homogeneous along two out of the three spatial directions, here

streamwise x and spanwise z direction. Therefore, the flow is only dependent on the wall-normal coordinate, and the perturbation has the following form:

$$\begin{aligned} \tilde{\boldsymbol{q}}(x,y,z,t) &= \hat{\boldsymbol{q}}(y)e^{i\Theta(x,z,t)} + c.c. \\ \Theta(x,z,t) &= \alpha x + \beta z - \omega t, \end{aligned} \tag{2}$$

where ω is the angular frequency, c.c. denotes the complex conjugate, and α, β are the wavenumbers in streamwise and spanwise direction, respectively.

Parabolized Stability Equations. A more general representation of the disturbances is given by:

$$\begin{aligned} \tilde{\boldsymbol{q}}(x,y,z,t) &= \hat{\boldsymbol{q}}(x,y)e^{i\Theta(x,z,t)} + c.c. \\ \Theta(x,z,t) &= \int_{x_0}^{x} \alpha(x')dx' + \beta z - \omega t. \end{aligned} \tag{3}$$

If a flow varies slowly in one spatial direction, say x, then a scale separation $1/Re$ is introduced between the weak variation in the x direction and the strong variation in the y direction. The normal basic flow velocity component and the streamwise dependence of the basic and disturbance flow scale with $1/Re$, where Re is based on a length scale l^* proportional to the boundary-layer thickness, $l^* = \sqrt{x^*\nu^*/U^*}$ ($*$ denotes dimensional quantities). With the above scaling and ansatz (3) introduced into the LNS equations, considering only terms that scale with powers of Reynolds number up to $1/Re$, we obtain the stability analysis approach based on PSE. The effects of small flow non-parallelism are consistently taken into account and due to the fact that the disturbance characteristics predicted by such a method are influenced by local and upstream flow conditions, this theory is called nonlocal. For a complete explanation about the PSE methodology, the readers are referred to Herbert [6]. Stability calculations were performed with the spatial nonlocal linear stability code NOLOT, which was developed in cooperation between DLR and the Swedish defence research agency FOI and has been extensively validated [7].

Adaptive Harmonic Linearized Navier-Stokes Methodology. The AHLNS equations are obtained in a similar way to the PSE formulation as regards the wave-like character of the disturbances which are divided into an amplitude function and wave function as Eq. (3). However, differently from the PSE approach, the streamwise wavenumber α and the amplitude function $\hat{\boldsymbol{q}}$ are allowed to vary rapidly in streamwise direction. The assumption of slowly varying flow in streamwise direction is removed also for the basic flow, so that all the terms of the LNS equations are kept. A multi-zonal approach is then applied, which exploits PSE relatively far away from the surface irregularity, where the streamwise variations of the basic flow and amplitude function are small, and AHLNS only in the vicinity of the irregularity. In the present paper, results obtained using this multi-zonal approach will be labeled as AHLNS results. For a detailed description of this methodology the readers are referred to Franco et al. [8].

Amplification Curve and Growth Rate. By integrating the spatial growth rate of the perturbations, the amplification curve of their amplitude along the streamwise direction can be obtained. The amplification curves of the DNS results presented in [2] allow a quantitative comparison with LST, PSE and AHLNS through the relation: $\ln(A_u/A_{ref})_{DNS} = \int_{x_{ref}}^{x} \sigma(x')dx'$, where A_u is the maximum amplitude along the wall-normal coordinate ($A_u(x) = \max_y |\hat{u}(x,y)|$) and σ is the spatial disturbance growth rate. In LST, the spatial growth rate is computed from the imaginary part of the complex streamwise wavenumber, $\sigma = -\alpha_i$. In PSE and AHLNS, it is given by $\sigma = -\alpha_i + \Re(\frac{1}{\xi}\frac{\partial \xi}{\partial x})$, where $\hat{u}$ at the wall-normal location where it reaches its maximum value, has been chosen in this paper among the possible choices for ξ. The growth rates of the DNS can also be determined carrying out numerically the differentiation of the amplification curves: $\sigma_{DNS} = d(\ln(A_u/A_{ref}))/dx$.

3 Results

3.1 Laminar Basic Flows

The laminar basic flows used in this work were computed by Tocci et al. [2] through DNS. The surface irregularities are located on a flat plate without pressure gradient at Reynolds number based on the centre position of the irregularity $Re_{x_c} = 4 \cdot 10^5$. The Blasius length scale $l_c^* = x_c^*/\sqrt{Re_{x_c}}$ at this location is chosen for non-dimensionalization. With this scaling, the center of the irregularities is located at $x_c = 632.46$. The non-dimensional height or depth of the geometric features is $h = 0.808$ ($Re_h = 511$) and the non-dimensional width of the humps and gap is $b = 31.62$ ($Re_b = 2 \cdot 10^4$). We refer the reader to [2] for further details on the basic flow characteristics. As example, Fig. 1 shows the steady laminar basic flow for one of the surface imperfections studied, a smooth hump.

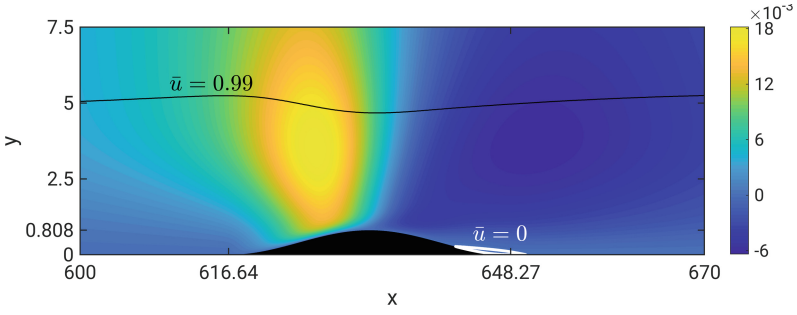

Fig. 1. Coloured contours of the non-dimensional wall-normal velocity component $\overline{v}$ and iso-lines of the non-dimensional streamwise velocity component $\overline{u} = 0.99$ (black) and $\overline{u} = 0$ (white). The axes are not to scale.

3.2 Instability Analysis

Before looking at the surface irregularities, the flat plate solution is considered in Fig. 2. The growth rate obtained from LST differs from the DNS and PSE calculations. This deviation can be explained by nonparallel effects, that is, the influence of growing boundary layer (see also [9]). Moreover, the amplitude curve of LST (Fig. 2, right) shows the integrated error, so that the relative deviation from DNS is higher far downstream. The curves for DNS and PSE of Fig. 2 essentially collapse and therefore show the remarkable agreement of the two numerical approaches in a flat plate boundary-layer flow. The growth rate of the DNS exhibits high values where the disturbances are introduced and thus manifest the generation of disturbances waves. Before considering the overall comparison of the methodologies, we point out some of the key findings concerning the applicability of LST and PSE in the presence of surface irregularities. Since the neutral point for the flat plate ($x = 620$) lies within the irregularities region (Fig. 1), a slighty upstream position ($x_{ref} = 610$) is chosen to normalize the amplitude in order to show the differences in amplification curves far downstream due to the irregularities only.

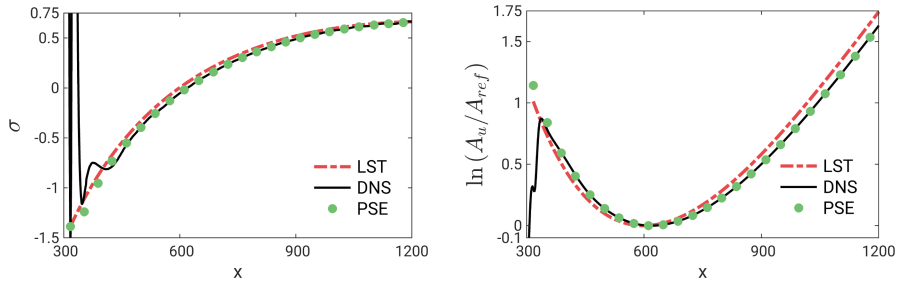

Fig. 2. Dimensional growth rates (left) and natural logarithm of the normalized disturbance amplitude (right) for TS waves at $\mathrm{F} = 2\pi f^* \nu^* / U_\infty^{*2} = 49.34 \cdot 10^{-6}$ in incompressible flat plate boundary-layer flow. A_{ref} represents the maximum amplitude of $\hat{u}$ along y at $x_{ref} = 610$.

LST. Particularly critical for the LST calculations is the region around a sharp edge, i.e. rectangular hump or step cases, where the LST computation stops. Basically, the resolution in streamwise direction for the LST can be the same as for the DNS and it is possible to achieve grid independence of the results. However, a small region in the vicinity of the sharp edge has to be omitted (see also [4]). For the forward-facing step, Fig. 3 shows the mesh independence study and the influence of the size of the region which is not considered for the LST computation, labelled with increasing size order as Δx_1, Δx_2 or Δx_3. Similar behaviour can be observed for the other irregularities with sharp edges, while for the smooth irregularities the LST computations could be carried out for all the points in streamwise direction.

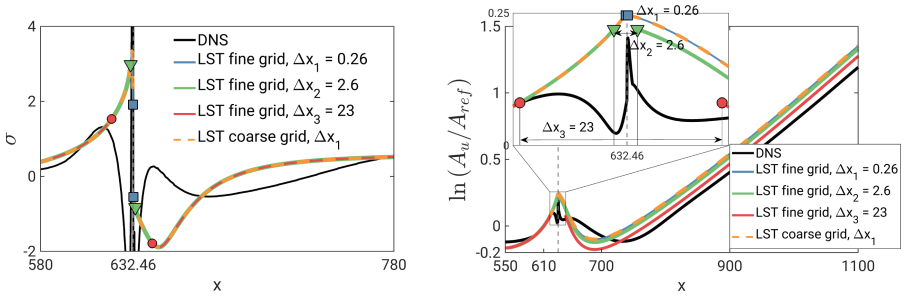

Fig. 3. Dimensional growth rates (left) and natural logarithm of the normalized disturbance amplitude (right) for TS waves at F $= 49.34 \cdot 10^{-6}$ in the presence of a forward-facing step. The dashed grey line shows the location of the step. The markers represent the last and first point of the splitted LST domains across the step: Δx_1, Δx_2 and Δx_3 refer to the increasing skipped region. A_{ref} represents the maximum amplitude of $\hat{u}$ along y at $x_{ref} = 610$.

PSE. The classical nonlocal stability equations, even though parabolized in the sense that second derivatives in the streamwise direction are missing, still contain some residual ellipticity. This leads to rapid oscillations of the solution which can eventually blow up the calculation when the marching step-size is too small. This step-size restriction becomes critical especially in the vicinity of the irregularity where higher resolution is needed. It is possible to march over the irregularity without a breakdown of the calculation only with large enough step-sizes. It can be shown that the residual ellipticity is mostly due to the upstream propagation through the streamwise pressure gradient terms. This issue can be then addressed through modifications of the PSE where the pressure gradient terms are neglected. Even though this technique relaxes the step-size restriction, it turns out that the grid convergence of the results can be obtained only for the smooth irregularities. For the smooth hump case the PSE results show an oscillatory behavior for $\alpha_r \cdot dx < 0.85$ and grid independence is not reached. Dropping the pressure terms allows grid independent results from a step size of $\alpha_r \cdot dx = 0.5$. On the contrary, the above procedure does not help in the presence of the rectangular hump and the forward-facing step. For those cases, it is worth mentioning that the PSE results are considerably affected not only by the step-size restriction, i.e. the number of points, but also by the distribution of the points where the PSE computation is done, especially in the vicinity of the irregularity. This is shown in Fig. 4 where the same number of points is considered but they are shifted such that one point falls right before or after the end of the hump. Figure 5 summarizes the PSE results for the irregularities studied, pointing out the problem of grid dependency in the presence of a sharp corner, i.e. rectangular hump and forward-facing step. We remind the reader that Andersson et al. [10] proposed another stabilization technique that removes the step-size restriction in PSE at the expense of an increasing artificial modification of the governing equations with decreasing step size, however it was not considered in this work.

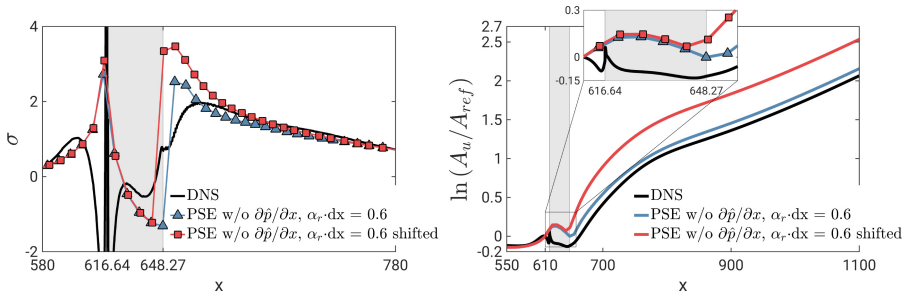

Fig. 4. Dimensional growth rates (left) and natural logarithm of the normalized disturbance amplitude (right) for TS waves at $F = 49.34 \cdot 10^{-6}$ in the presence of a rectangular hump, indicated by the grey area. The markers represent the point distribution for the PSE computations. A_{ref} represents the maximum amplitude of $\hat{u}$ along y at $x_{ref} = 610$.

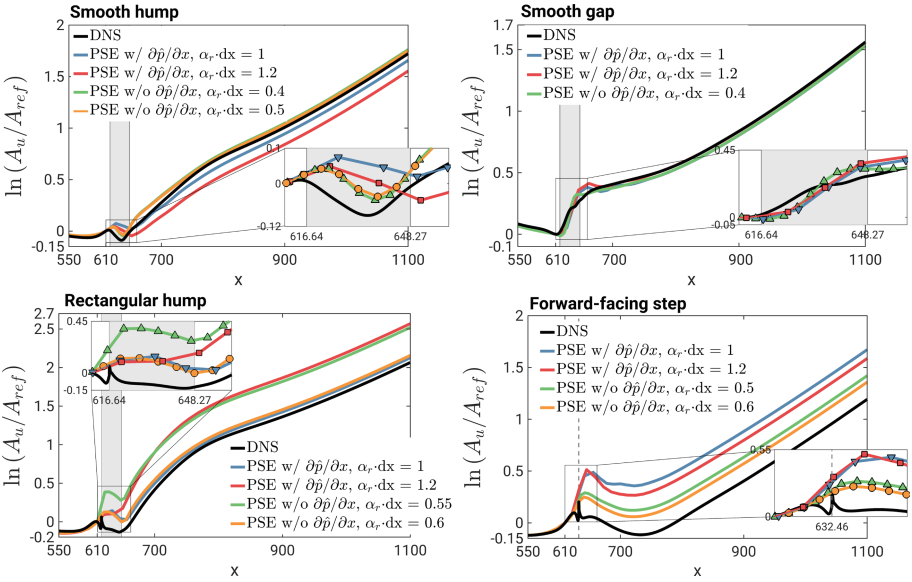

Fig. 5. Natural logarithm of the normalized disturbance amplitude for TS waves at $F = 49.34 \cdot 10^{-6}$. The grey area indicates the location of the humps and gap, while the dashed grey line shows the location of the step. A_{ref} represents the maximum amplitude of $\hat{u}$ along y at $x_{ref} = 610$.

The comparison between LST, PSE, AHLNS and DNS is shown in Fig. 6 for a rectangular and smooth hump, smooth gap and forward-facing step. A rectangular gap and a backward-facing step were also investigated; however, their instability analyses do not provide any further conclusion which is not already drawn by analysing the other cases, therefore they are omitted here due to

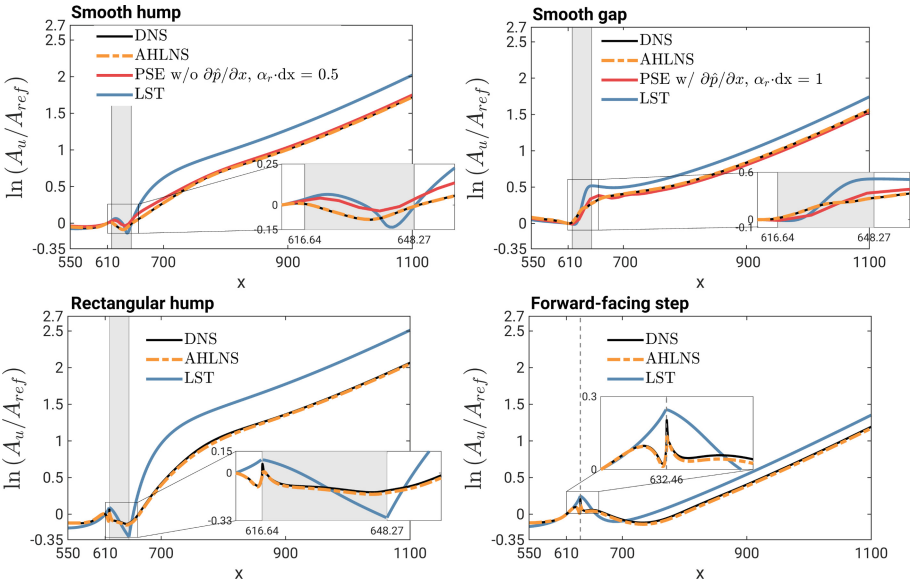

Fig. 6. Natural logarithm of the normalized disturbance amplitude for TS waves at $F = 49.34 \cdot 10^{-6}$. The grey area indicates the location of the humps and gap, while the dashed grey line shows the location of the step. A_{ref} represents the maximum amplitude of $\hat{u}$ along y at $x_{ref} = 610$.

space limitation. The AHLNS amplification curves are in excellent agreement with those obtained by DNS for all the surface irregularities, demonstrating the validity of this methodology to study the effect of surface irregularities on the spatial development of convective boundary-layer instabilities. PSE is able to predict the development of TS waves over the smooth hump and gap with some deviations in the region of the irregularities which, anyway, do not cause large differences far downstream where the same growth rate of the flat plate is recovered. As mentioned earlier, the smooth hump case required to drop the pressure terms $\partial\hat{p}/\partial x$ in order to reduce the step size and achieve a converged solution. The latter stabilization technique was not necessary for the smooth gap while for the rectangular hump and forward-facing step the results were anyway grid dependent (see Fig. 5) and therefore the PSE curves are not plotted. For all investigated cases, LST is over-predicting the growth in the area of the separation bubble induced by the irregularities. As a result, the amplification level far downstream is higher compared to DNS. For LST, the basic state is approximated as locally parallel, an assumption that does not hold, in particular in the vicinity of the irregularity where the flow is deflected reaching higher value of the wall-normal velocity (Fig. 1). Besides violating the nonparallel assumption, the local distortion of the boundary layer induced by the irregularities might conflict with the PSE requirement of a slowly changing basic flow in the streamwise direction. As expected, the rectangular hump introduces stronger localized

streamwise gradients compared to the smooth hump, as shown in Fig. 7 where the derivative $\partial\overline{u}/\partial x$ is plotted. In Fig. 8 the ratio between the maximum along the wall-normal direction of the derivative $\partial\overline{u}/\partial x$ and $\partial\overline{u}/\partial y$ gives an indication of the regions where actually the gradients in the streamwise direction are not negligible compared to that in the wall-normal direction. In the rectangular hump and forward-facing step cases, the peaks associated with high values of this ratio should cast doubt on the applicability of PSE and provide an explanation for the difficulties in obtaining grid-converged solutions (Fig. 4 and Fig. 5).

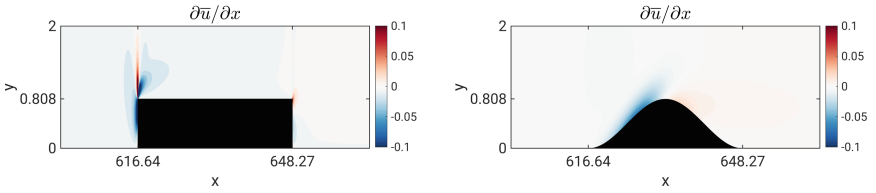

Fig. 7. Coloured contours of the non-dimensional streamwise derivative of the streamwise velocity component for the basic flow $\overline{u}$ (the axes are not to scale). Rectangular hump (left) and smooth hump (right).

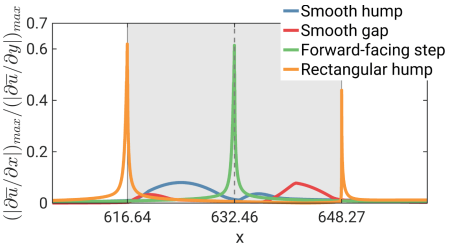

Fig. 8. Ratio of the streamwise and wall-normal derivative of the streamwise velocity component of the basic flow $\overline{u}$. The light grey area indicates the location of the humps and gap, while the dashed dark grey line shows the location of the step.

LST and PSE required a similar computational effort of the order of seconds. The AHLNS computations took around minutes and come at a fraction of the cost of DNS which are orders of magnitude more expensive.

4 Conclusions

The spatial linear instability analysis of TS waves is presented through the results provided by LST, PSE and AHLNS in the presence of different 2-D irregularities on a flat plate in an incompressible flow. Even if limited to a single frequency, comparison with DNS allows to evaluate the accuracy and applicability of the

different approaches. The AHLNS approach, given the excellent agreement with DNS for all the cases, proves to be a perfectly suited tool for the boundary-layer instability analysis in the presence of large streamwise gradients. Moreover, with a moderate computational effort compared to DNS, it is well suited for parametric studies. The use of PSE should be avoided in the presence of sharp corners, where the assumption of slowly varying basic flow with respect to x is violated but it could still be valid for smooth irregularities such as the ones studied here. However, we remind the reader that PSE could also provide wrong spatial amplification in the presence of smooth irregularities if they introduce stronger streamwise gradients. In general, PSE requires some attention due to its step-size restriction with respect to the resolution required in the vicinity of the irregularities. In this regard, the smooth gap is the less critical irregularity while the smooth hump case required to neglect the pressure terms $\partial\hat{p}/\partial x$ in order to reduce the step size and achieve grid convergence. Besides these pure numerical considerations, one should always keep in mind that when the characteristic length scale of the perturbation in the streamwise direction, i.e. the TS wavelength, is of the same order as the corresponding characteristic length scale of the streamwise flow variation induced by the surface irregularity, the applicability of PSE is dubious. LST shows differences from the DNS results in all the cases studied. This disagreement is entirely due to the inherent weaknesses of the LST modelling assumptions in the presence of surface irregularities which induce local distortion of the boundary layer.

Acknowledgements. The financial support of SSeMID, Stability and Sensitivity Methods for Industrial Design, funded by European Union's Horizon 2020 research and innovation programme under the Marie Skłodowska-Curie Grant Agreement No. 675008, and from the Clean Sky 2 Joint Undertaking under the European Union's Horizon 2020 research and innovation programme under Grant Agreement No. CS2-AIR-GAM-2014-2015-01 are gratefully acknowledged.

References

1. Nenni, J.P., Gluyas, G.L.: Aerodynamic design and analysis of an LFC surface. Astronaut. Aeronaut. **4**(7), 52–57 (1966)
2. Tocci, F., Chauvat, G., Hein, S., Hanifi, A.: Direct numerical simulations of Tollmien-Schlichting disturbances in the presence of surface irregularities (To appear in Procedia IUTAM, 2020)
3. Franco, J.A., Hein, S., Valero, E.: On the influence of two-dimensional hump roughness on laminar-turbulent transition. Phys. Fluids **32**, 034102 (2020)
4. Edelmann, C., Rist, U.: Impact of forward-facing steps on laminar-turbulent transition in transonic flows. AIAA J. **53**(9), 2504–2511 (2015)
5. Park, D., Oh, S.: Effect of shape of two-dimensional smooth hump on boundary layer instability. Int. J. Aeronaut. Space Sci. (2020)
6. Herbert, T.: Parabolized stability equations, Progress in Transition Modelling, AGARD Report No. 793 (1994)
7. Hein, S., Bertolotti, F.P., Simen, M., Hanifi, A., Henningson, D.: Linear nonlocal instability analysis - the linear NOLOT Code. DLR-IB 223–94 A56 (1995)

8. Franco, J.A., Hein, S.: Adaptive Harmonic Linearized Navier-Stokes equations used for boundary layer instability analysis in the presence of large streamwise gradients. AIAA Paper 2018-1548 (2018)
9. Fasel, H., Konzelmann, U.: Non-parallel stability of a flat-plate boundary layer using the complete Navier-Stokes equations. J. Fluid Mech. **221**, 311–347 (1990)
10. Andersson, P., Henningson, D., Hanifi, A.: On a stabilization procedure for the parabolic stability equations. J. Eng. Math. **33**, 311–332 (1998)